Chinese Chemical Letters 35 (2024) 109002

Contents lists available at ScienceDirect

Chinese Chemical Letters

journal homepage: www.elsevier.com/locate/cclet

Interfacial charge redistribution to promote the catalytic activity of Vs-CoP-CoS_2/C n-n heterojunction for oxygen evolution

Jiawen Sun, Hui Xue*, Jing Sun, Niankun Guo, Tianshan Song, Yi-Ru Hao, Qin Wang*

College of Chemistry and Chemical Engineering, Inner Mongolia University, Hohhot 010021, China

ARTICLE INFO

Article history:
Received 7 July 2023
Revised 10 August 2023
Accepted 28 August 2023
Available online 4 September 2023

Keywords:
Charge redistribution
n-n Heterojunction
Built-in electric field
Sulfur vacancy
Oxygen evolution reaction

ABSTRACT

Modulating surface charge redistribution based on interface and defect engineering has been considered as a resultful means to boost electrocatalytic activity. However, the mechanism of synergistic regulation of heterojunction and vacancy defects remains unclear. Herein, a Vs-CoP-CoS_2/C n-n heterojunction with sulfur vacancies is successfully constructed, which manifests superior electrocatalytic activity for oxygen evolution, as demonstrated by a low overpotential of 170 mV to reach 10 mA/cm^2. The experimental results and density functional theory calculations testify that the outstanding OER performance of Vs-CoP-CoS_2/C heterojunction is owed to the synergistic effect of sulfur vacancies and built-in electric field at n-n heterogeneous interface, which accelerates the electron transfer, induces the charge redistribution, and regulates the adsorption energy of active intermediates during the reaction. This study affords a promising means to regulate the electrocatalytic performance by the construction of heterogeneous interfaces and defects, and in-depth explores the synergistic mechanisms of n-n heterojunction and vacancies.

The accelerated consumption of fossil fuels has led to energy crisis and environmental pollution, and the pursuit of environmentally-friendly and renewable energy has become a top priority [1–3]. Electrochemical water splitting provides a promising and sustainable method for large-scale production of clean and efficient hydrogen energy without environmental cost [4–6]. As a significant half-reaction, the oxygen evolution reaction (OER) plays a crucial role in various renewable energy storage and conversion devices, such as hydrogen-producing water splitting, regenerative fuel cells, and metal-air batteries [7,8]. Nevertheless, the complex four-electron coupled proton reaction kinetics of OER is slow and requires a high overpotential, which is a major factor limiting the efficiency of water electrolysis [9,10]. Up to now, noble metals oxides like IrO_2 and RuO_2 have been considered as the first-rank OER catalysts, while their commercial application on a large scale is severely limited by the high cost and scarcity [11–13]. Therefore, developing OER electrocatalysts with superior activity, good chemical stability and cost-effective is urgent.

Over the past few years, efforts have been devoted to investigating terrestrially abundant transition metal compounds such as oxides, sulfides, selenides, and phosphides as efficient OER electrocatalysts [14–16]. Transition metal phosphides (TMPs) are known for their low kinetic energy barrier and excellent electrical conductivity [17–20]. Many studies have shown that TMPs tend to exhibit excellent hydrogen evolution reaction (HER) activity, while the OER performance of these TMPs catalysts is often unsatisfactory [21–23]. As a consequence, the enhancement of the OER electrocatalytic performance of TMPs is still a research hotspot. The efficient integration of single-component catalysts to synthesize heterojunctions is a valid method to boost the catalytic activity of transition metal-based catalysts [24,25]. The formation of heterogeneous interfaces can effectively promote the interfacial electron transport, tailor the electronic structure, and regulate the adsorption free energy of the reaction species, thereby significantly improve the electrocatalytic activity [26,27]. Accordingly, as a typical type of heterojunction, n-n heterojunction catalysts have made significant progress in the field of batteries due to their ability to accelerate charge transfer and excellent performance [28]. Moreover, from the perspective of semiconductor physics, two n-type semiconductors with different energy structures coming into contact and reaching thermodynamic equilibrium will induce the formation of a built-in electric field and two opposite charge distribution regions at the interface [29,30], which is beneficial to the rapid transfer of electrons between n-n type semiconductors in the catalytic process, and improving the catalytic activity [30]. Based on this, n-type semiconductor TMPs are combined with another n-type semiconductor to form n-n type heterojunctions, and the interfacial electronic regulation based on the built-in electric field is

* Corresponding authors.
E-mail addresses: hxue@imu.edu.cn (H. Xue), qinwang@imu.edu.cn (Q. Wang).

https://doi.org/10.1016/j.cclet.2023.109002
1001-8417/

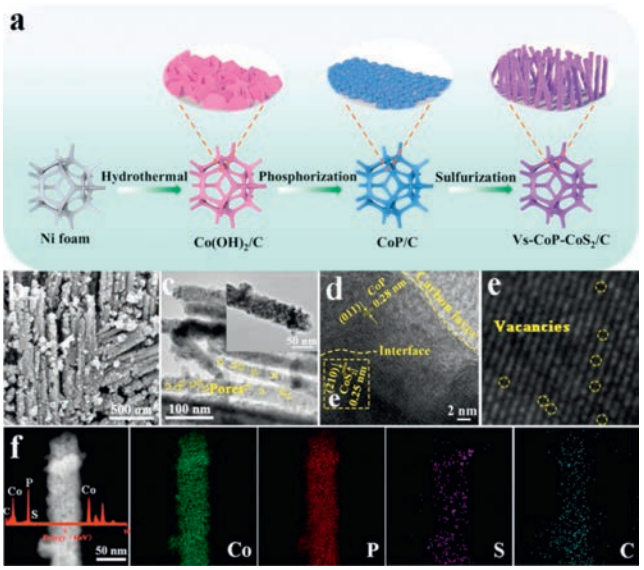

Fig. 1. (a) Schematic illustration of the formation of Vs-CoP-CoS_2/C. (b) SEM, (c) TEM, (d, e) HRTEM, (f) STEM (inset: the EDS spectrum) and the corresponding elemental mappings of Co, P, S and C of Vs-CoP-CoS_2/C.

expected to significantly improve their electrocatalytic activity for OER.

In addition to constructing heterostructures, the fabrication of defects in the crystal structure is also a valid method to improve the electrocatalytic performance [31]. The effect of vacancy defects in electrocatalysts on OER performance has been extensively studied [32]. In general, the introduction of defects can tailor the electronic structure and charge distribution of atoms, increase the active sites for the reaction, and thus enhancing the intrinsic activity of the catalysts [33,34]. Among them, anion vacancies, as an important solid defect, can promote the OER performance by improving the electrical conductivity and surface activity of the electrocatalysts [35,36]. For instance, Kang and co-workers proposed that sulfur (S) vacancies can modulate the electronic structure of $CuCo_2S_4$ and promote the intrinsic conductivity, thus enhancing the electrocatalytic activity [37]. Therefore, combining the advantages of vacancy defects to construct an n-n type semiconductor heterojunction system is expected to further boost the electrochemical OER performance of TMPs.

Herein, a Vs-CoP-CoS_2/C n-n heterojunction nanorods with abundant sulfur vacancies has been successfully constructed. Notably, the as-prepared Vs-CoP-CoS_2/C heterojunction manifests superior electrocatalytic activity for oxygen evolution, as demonstrated by a low overpotential of 170 mV and a minor Tafel slope of 39 mV/dec to reach 10 mA/cm^2. Combined with experimental results and density functional theory calculations, the outstanding OER performance of Vs-CoP-CoS_2/C heterojunction is owed to the synergistic effect of sulfur vacancies and built-in electric field at n-n heterogeneous interface, which accelerates the electron transfer, induces the charge redistribution, and regulates the adsorption energy of active intermediates during the reaction. This study affords a promising means to regulate the electrocatalytic performance by the construction of heterogeneous interfaces and defects, and in-depth explores the synergistic mechanisms of n-n heterojunction and vacancies.

The synthesis process of Vs-CoP-CoS_2/C heterojunction is shown in Fig. 1a. Briefly, the $Co(OH)_2$/C precursor was prepared by hydrothermal method on nickel foam and then treated with phosphating and sulfidation to obtain Vs-CoP-CoS_2/C heterojunction. Fig. S1 (Supporting information) displays the results of X-ray diffraction (XRD) on the crystal phase structure and composition of the Vs-CoP-CoS_2/C heterojunction. The diffraction peaks located at 36.3°, 48.1°, 52.2°, and 56.1° are attributed to the (111), (211), (103), and (020) planes of CoP (JCPDS No. 65–2593), respectively. In addition, the diffraction peaks at 32.3°, 36.3°, 39.9°, and 46.4° belong to (200), (210), (211), and (220) facets of CoS_2 (JCPDS No. 65–3322). The XRD results demonstrate that CoP and CoS_2 phases have been successfully synthesized. The morphology of the electrocatalysts was analyzed by SEM. The nanorods morphology of Vs-CoP-CoS_2/C has been clearly observed in Fig. 1b, and the morphologies of contrast samples, such as $Co(OH)_2$, $Co(OH)_2$/C, CoP/C, and CoS_2/C are also provided in Fig. S2 (Supporting information). The results show that phosphating and sulfurization have great influence on the lamellar morphology of $Co(OH)_2$/C precursor. Many pores on the surface of Vs-CoP-CoS_2/C heterojunction can be detected from the TEM image (Fig. 1c), which can increase the specific surface area, facilitate the exposure of the active site inside the Vs-CoP-CoS_2/C and direct contact with the reactants, thus significantly improving the catalytic activity. The HRTEM image (Fig. 1d) clearly discloses the carbon layer structure in the Vs-CoP-CoS_2/C heterojunction. The presence of carbon layer on the surface can effectively enhance the electron conduction of the electrocatalysts. Moreover, the lattice distance of 0.28 nm matches well with the (011) plane of CoP and 0.25 nm is ascribed to the (210) plane of CoS_2, respectively. Importantly, a clear heterojunction interface can be observed, confirming the Vs-CoP-CoS_2/C n-n heterojunction is successfully obtained. The formation of heterojunctions can facilitate the charge transfer and accelerate the reaction kinetics. Meanwhile, many atomic discontinuities can be detected in the CoS_2 lattice of Vs-CoP-CoS_2/C heterojunction, which may result from the formation of S vacancies during sulfide synthesis (Fig. 1e). Besides, the HAADF-STEM images (Fig. 1f) and the corresponding elemental mapping reveal that the elements of Co, P, S, and C are uniformly dispersed in the Vs-CoP-CoS_2/C nanorods.

The electron effect between CoP/C and CoS_2/C and surface element valence states of catalysts was studied through X-ray photoelectron spectroscopy (XPS). As depicted in Fig. 2a, the survey spectrum shows the presence of Co, P, S, C, and O elements in Vs-CoP-CoS_2/C catalyst. The Co 2p core level spectrum (Fig. 2b) can be deconvoluted into six peaks, corresponding to Co^{3+} (779.2/794.1 eV), Co^{2+} (782.1/797.9 eV), and satellite peaks (786.6/803.5 eV) of Co $2p_{3/2}$ and Co $2p_{1/2}$, respectively [38–40]. Interestingly, the binding energy of Co 2p in Vs-CoP-CoS_2/C heterostructure is positively shifted by 0.6 eV relative to CoP/C and negatively shifted by 0.5 eV relative to CoS_2/C. The results indicate that there is a strong electron interaction between CoP/C and CoS_2/C, and continuous electron transfer between them is beneficial to significantly tailor the electronic structure of metal Co center [41]. In the P 2p spectrum (Fig. 2c), the P-Co bond with the binding energies of 129.7 eV and 130.5 eV and P-O bond located at 134.2 eV can be deconvoluted [42,43]. It is also observed that the peak of P-Co is positively shifted by 0.3 eV compared to CoP/C. In Fig. 2d, the S 2p spectrum of Vs-CoP-CoS_2/C displays the S $2p_{3/2}$ (161.9 eV) and S $2p_{1/2}$ (163.0 eV) [44], which are negatively shifted by 0.6 eV compared to CoS_2/C. In addition, the presence of the S^{2-} peak may be due to the generation of S vacancies as reported in the literatures [45]. The remaining two peaks, 168.9 eV and 170.1 eV belong to the S-O bond [46]. The O 1s spectrum of Vs-CoP-CoS_2/C can be deconvoluted into two peaks located at 531.9 eV and 533.0 eV, which are ascribed to O–H and water adsorption, respectively (Fig. S3a in Supporting information) [47]. The C 1s spectrum of Vs-CoP-CoS_2/C exhibits three peaks of C–C, C–O, and C=O (Fig. S3b in Supporting information) [48]. Based on the above analysis, the change in binding energy reveals a redistribution of charge in the Vs-CoP-CoS_2/C heterogeneous interface, and the spontaneous transfer of electrons from CoP/C to CoS_2/C, result-

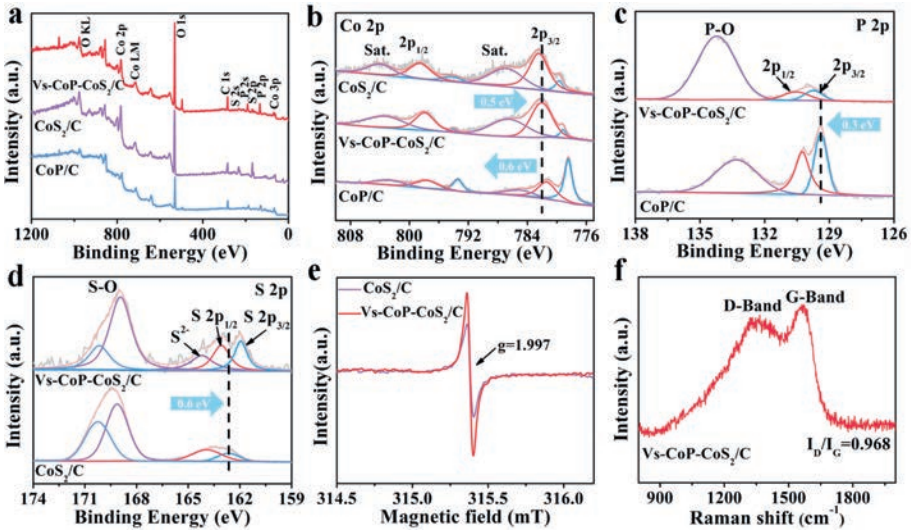

Fig. 2. XPS spectra of the obtained electrocatalysts: (a) Survey spectra, (b) Co 2p, (c) P 2p and (d) S 2p, (e) EPR spectra of the CoS_2/C and Vs-CoP-CoS_2/C. (f) Raman spectrum of Vs-CoP-CoS_2/C.

ing in hole accumulation on the CoP/C side, which in turn significantly promotes the OER reaction [27]. Furthermore, the electron paramagnetic resonance (EPR) provides strong evidence for the existence of S vacancies in the CoP-CoS_2/C. As depicted in Fig. 2e, the EPR signal is observed at $g = 1.997$, which is attributed to the unpaired electrons [45]. Compared with CoS_2/C, the signal intensity of Vs-CoP-CoS_2/C is significantly enhanced, indicating an increase in S vacancies. Therefore, according to the results of EPR, XPS, and TEM, there are a large number of S vacancy defects in Vs-CoP-CoS_2/C catalyst. The Raman spectroscopy was further performed to analyze the structure of the Vs-CoP-CoS_2/C catalyst. It can be seen from Fig. 2f that the intensity ratio of D band and G band (I_D/I_G) of Vs-CoP-CoS_2/C is 0.968, showing a high degree of graphitization and electrical conductivity, which is conducive to the improvement of catalytic activity [49].

The OER catalytic activity of the samples was detailedly studied in 1 mol/L KOH solution using a typical three-electrode electrochemical system. The influence of sulfurization degree on the OER activity was explored by adjusting the sulfurization time. The results indicate that the optimal OER activity of Vs-CoP- CoS_2/C catalyst was achieved when the sulfurization time was 60 min (Figs. S4 and S5 in Supporting information). Specifically, the LSV curves show that the overpotentials for Vs-CoP-CoS_2/C, CoS_2/C, CoP/C, and the commercial IrO_2/NF are 170, 190, 230, and 330 mV, respectively (Fig. 3a). Obviously, the Vs-CoP-CoS_2/C catalyst possesses the optimal OER activity. Besides, the OER overpotential (193 mV) of Vs-CoP-CoS_2 catalyst (without carbon layer) is also lower than Vs-CoP-CoS_2/C, indicating that graphitic carbon could enhance the conductivity and improve the OER catalytic performance (Fig. S6 in Supporting information). In addition, the Tafel slope of 39 mV/dec for Vs-CoP-CoS_2/C catalyst, lower than those of CoS_2/C (45 mV/dec), CoP/C (50 mV/dec), and IrO_2/NF (62 mV/dec), indicating a fast OER kinetics for the Vs-CoP-CoS_2/C catalyst (Figs. 3b and c). Furthermore, at the overpotential of 350 mV, the turnover frequency (TOF) value of 0.72 s^{-1} for Vs-CoP-CoS_2/C catalyst is also higher than that of CoS_2/C (0.25 s^{-1}) and CoP/C (0.18 s^{-1}) in Fig. S7a (Supporting information). The charge-transfer properties of the obtained samples were further investigated by measuring the electrochemical impedance spectroscopy (EIS). The smallest charge transfer resistance (R_{ct}) for Vs-CoP-CoS_2/C indicates the fastest kinetic rate of OER (Fig. 3d). The excellent OER electrocatalytic activity of Vs-CoP-CoS_2/C was further demonstrated by measuring the C_{dl} of the catalyst through cyclic voltammetry (CV) in the non-Faraday region. According to the CV curve (Fig. S8 in Supporting information), the C_{dl} value of the Vs-CoP-CoS_2/C is 28 mF/cm^2, which is larger than that of CoS_2/C (26 mF/cm^2) and CoP/C (16 mF/cm^2) (Fig. 3e). In addition, the electrochemically active surface area (ECSA) of the samples can be reflected by the C_{dl}, and the highest ECSA of 700 cm^2 for the Vs-CoP-CoS_2/C catalyst indicates more active sites are exposed on the catalyst surface (Fig. S7b in Supporting information). These results shows that the construction of heterojunction and S vacancies are beneficial to improve the OER electrocatalytic activity. On the other hand, stability is another important indicator for estimating the performance of electrocatalysts. The OER stability of Vs-CoP-CoS_2/C was tested by *i-t* chronoamperometry and CV cycles. It can be seen from Fig. 3f that the *i-t* curve has no obvious current density loss after 20 h. Besides, the polarization curves after 1000 CV cycles also show negligible loss of activity (inset in Fig. 3f), which further confirms its excellent electrochemical stability. Moreover, comparison with recently reported OER catalysts further demonstrates the excellent OER catalytic activity of the Vs-CoP-CoS_2/C (Fig. 3g and Table S1 in Supporting information). The electrochemical test of overall water splitting is shown in Fig. S9 (Supporting information), the overpotential of the Vs-CoP-CoS_2/C||Vs-CoP-CoS_2/C system in 1 mol/L KOH solution is 287 mV at 10 mA/cm^2, and it can be maintained for 24 h without performance attenuation.

In order to reveal the underlying reason for the enhanced OER electrocatalytic activity of the Vs-CoP-CoS_2/C heterojunction, and in-depth explore the interaction between CoP/C and CoS_2/C, ultraviolet photoemission spectroscopy (UPS) tests were performed to establish the corresponding energy level diagrams. In Figs. 4a and b, the Mott-Schottky plots of CoP/C and CoS_2/C exhibit positive slopes, which are typical for n-type semiconductors [28,50]. It is demonstrated that an n-n heterojunction between CoP/C and CoS_2/C has been formed. The synthesis of multicomponent heterostructures can implement the regulation of the d-band center, which can be calculated based on the UPS results. In Fig. 4c, the obtained d-band center of CoP/C, CoS_2/C, and Vs-CoP-CoS_2/C are −4.98, −4.94, and −4.92 eV, respectively, indicating the Vs-CoP-CoS_2/C sample shifts up closer to Fermi level than those of CoP/C and CoS_2/C. In general, the d-band center with relation to the binding strength of the reaction intermediates. The upward shift of d-band center indicates that the binding strength between catalyst

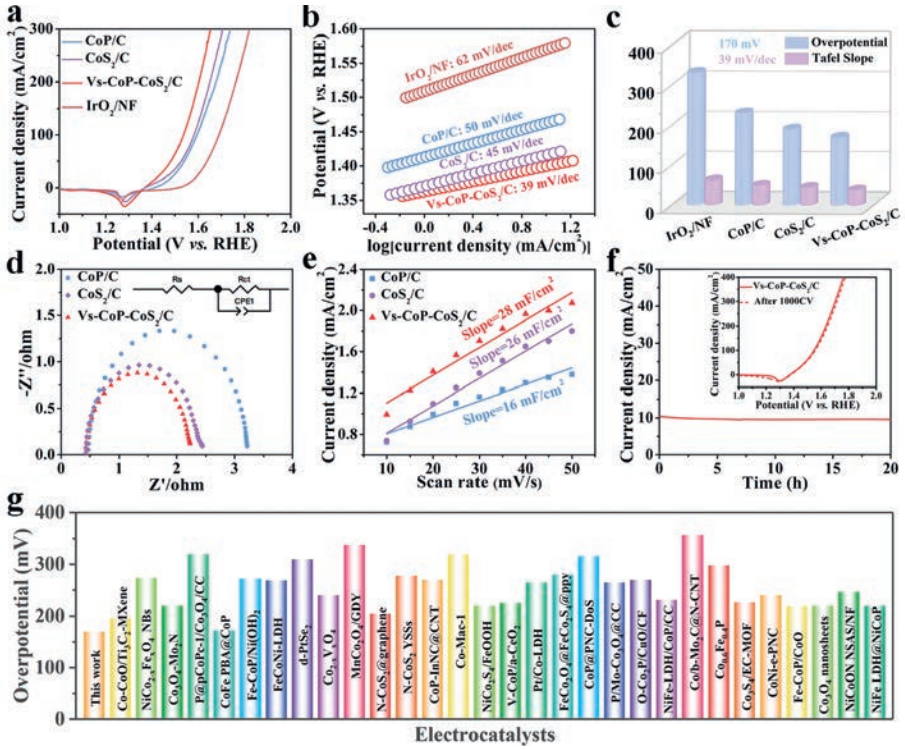

Fig. 3. (a) OER polarization curves. (b) Tafel slopes. (c) Histogram of the overpotentials and Tafel slopes. (d) Nyquist plots. (e) $C_{dl.}$ (f) Chronopotentiometric durability test (inset: LSV curves of Vs-CoP-CoS_2/C before and after 1000 cycles). (g) A recently reported comparison of OER electrocatalysts at 10 mA/cm^2.

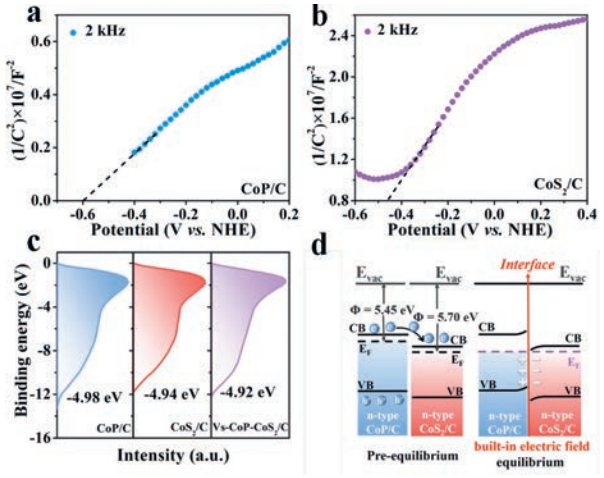

Fig. 4. Mott-Schottky plots of (a) CoP/C and (b) CoS_2/C at 2000 Hz. (c) UPS spectra of CoP/C, CoS_2/C, and Vs-CoP-CoS_2/C. (d) Per-equilibrium and equilibrium states of Vs-CoP-CoS_2/C n-n heterojunction (E_{vac} = vacuum energy, CB = conduction band, VB = valence band, E_F = Fermi level, and Φ = work function).

and intermediate is enhanced, which is beneficial to reducing the potential barrier and boosting the OER catalytic activity [51]. The interfacial charge polarization and band structure alteration were further analyzed by using UPS in Fig. S10 (Supporting information). The equation: $\Phi = h\nu$ - $E_{Cutoff} + E_F$ can be used to calculate the work function (Φ), where hν and E_F are 21.2 eV and 0 eV. Thus, the Φ values of CoP/C and CoS_2/C are 5.45 eV and 5.70 eV, respectively. Besides, the valence band (VB) values of CoP/C and CoS_2/C are 1.84 eV and 1.88 eV (inset in Fig. S10), respectively. In order to study charge transfer between CoP/C and CoS_2/C, the energy band diagrams before and after contact are provided (Fig. 4d). Because of the difference in Fermi levels, electrons flow from CoP/C to CoS_2/C until they reach a Fermi equilibrium, resulting in the formation of the built in electric field and a space charge region. Importantly, the built-in electric field facilitates interfacial electron transport and enhances electrical conductivity [52]. In addition, the formation of positively charged active centers on the surface of CoP/C promotes the migration of OH^- in alkaline electrolytes and improves the adsorption capacity of CoP/C to OH^-, thus promoting the OER process.

DFT calculations were used to further study the OER catalytic performance enhancement of n-n heterojunction and sulfur vacancy. We first calculate four models including two single components, sulfur vacancy-free heterojunction, and sulfur vacancy-containing heterojunction, which are represented by CoP/C, CoS_2/C, CoP-CoS_2/C, and Vs-CoP-CoS_2/C, respectively (Figs. 5a-c and Fig. S11 in Supporting information). The OER performance of electrocatalyst is strongly correlated with the chemisorption energy of the surface oxygen-containing intermediates, such as *OH, *O, and *OOH [35,53]. Therefore, we studied the configuration and Gibbs free energy changes of oxygen-containing intermediates on the catalyst surface. As can be seen from Fig. 5d and Fig. S12 (Supporting information), the rate-determining step during the OER process of CoP/C, CoS_2/C, CoP-CoS_2/C, and Vs-CoP-CoS_2/C is *OOH adsorption with free energies of 2.12, 1.97, 1.86, and 1.74 eV, respectively. It is well known that lower variations in the free energy of rate-determining steps favor OER thermodynamics. Therefore, the construction of heterojunction and sulfur vacancies can provide abundant active sites, reduce the energy barrier, and promote OER kinetics. Since the OER activity is concerned with the d-orbital of the transition metal active center, the corresponding projected density of state of the 3d-band of Co is calculated [54,55]. As shown in Fig. 5e and Fig. S13 (Supporting information), the 3d-band center of Vs-CoP-CoS_2/C shifts obviously to a higher energy level comparing with CoP/C, CoS_2/C, and CoP-CoS_2/C, indicating that *OH, *O, and *OOH have stronger binding strength with the catalyst, which is in good agreement with the experimental results. The work functions

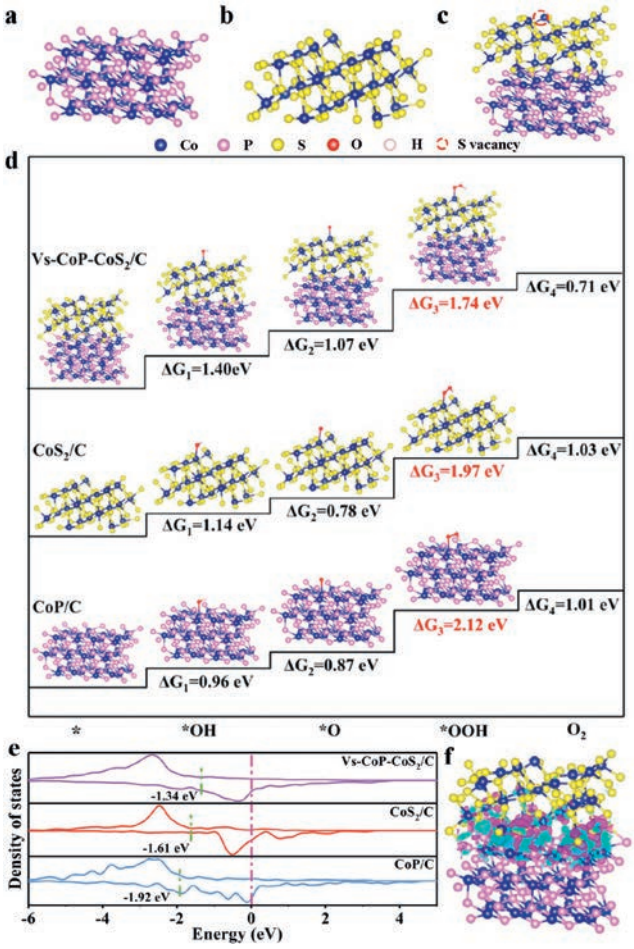

Fig. 5. Optimized models (a) CoP/C, (b) CoS_2/C, and (c) Vs-CoP-CoS_2/C. (d) Gibbs free energy changes diagram of CoP/C, CoS_2/C and Vs-CoP-CoS_2/C. (e) Calculated DOS of CoP/C, CoS_2/C, and Vs-CoP-CoS_2/C. (f) Charge density difference in the interface of Vs-CoP-CoS_2/C (The bule and red represent charge dissipation and aggregation in the space, respectively).

of CoP/C and CoS_2/C surfaces are 5.34 eV and 5.59 eV, respectively, and the electrons will be transferred from CoP/C to CoS_2/C until the two Fermi energies are aligned (Fig. S14 in Supporting information). The electron density difference of CoP-CoS_2/C is shown in Fig. S15 (Supporting information). It can be observed that charged active centers are generated at the n-n heterogeneous interface, further manifesting the rapid and continuous charge transfers from CoP/C to CoS_2/C [56,57]. While the electron aggregation and dissipation of Vs-CoP-CoS_2/C (Fig. 5f) increased in the n-n junction region, indicating that the introduction of sulfur vacancy can enhance electron transfer more effectively. From the above calculation results, the n-n junction and S vacancies formed in Vs-CoP-CoS_2/C sample can accelerate the electron transfer, induce the charge redistribution [58], regulate the adsorption/desorption energy of intermediates, thereby significantly enhancing the electrocatalytic activity for OER.

Based on the above experimental results and theoretical analysis, the prepared Vs-CoP-CoS_2/C n-n heterojunction has superior OER activity, which is mainly attributed to the following aspects: (1) The formed built-in electric field at the interface of CoP/C and CoS_2/C can boost electron transfer and tailor the electronic structure of metal Co; (2) The abundant S vacancies not only enhance the adsorption capacity of the catalyst to the reaction intermediates, but also further boost electron transfer, thus significantly improving the catalytic activity; (3) The highly graphitized carbon

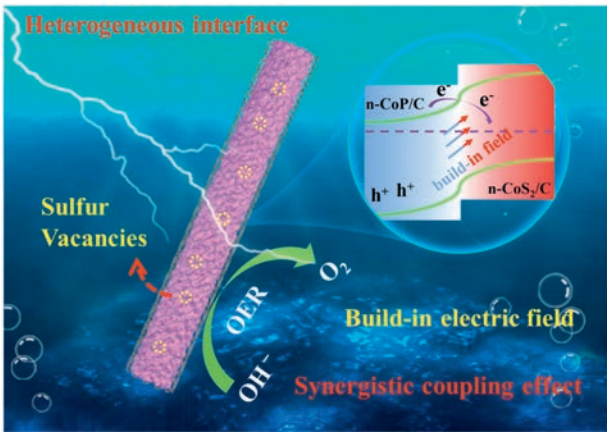

Scheme 1. Illustration of catalytic mechanism for Vs-CoP-CoS_2/C.

layer in Vs-CoP-CoS_2/C n-n heterojunction can increase the electrical conductivity, which is conducive to the electrocatalytic OER (Scheme 1).

In summary, we successfully synthesized an efficient Vs-CoP-CoS_2/C n-n heterojunction. Benefiting from the charge redistribution and S vacancies, the Vs-CoP-CoS_2/C catalyst exhibits excellent OER electrocatalytic activity with an overpotential low to 170 mV at 10 mA/cm^2. DFT calculations prove that n-n heterogeneous interface and S vacancies are beneficial to accelerate the electron transfer, induce the charge redistribution, and regulate the Gibbs free energy of reactive species. This study affords a promising method to optimize the electrocatalytic activity by the construction of heterogeneous interfaces and vacancy defects.

Declaration of competing interest

There are no conflicts to declare.

Acknowledgments

This project was financially supported by the National Natural Science Foundation of China (NSFC, Nos. 22269015, U22A20107, 22205119) and Natural Science Foundation of Inner Mongolia Autonomous Region of China (Nos. 2021ZD11, 2019BS02015).

Supplementary materials

Supplementary material associated with this article can be found, in the online version, at doi:10.1016/j.cclet.2023.109002.

References

[1] H. Ding, H.F. Liu, Y. Xie, et al., Chem. Rev. 121 (2021) 13174–13212.
[2] X. Tian, X.F. Lu, X.W. Lou, et al., Joule 4 (2020) 45.
[3] B. Wu, H.B. Meng, T. Petit, et al., Adv. Funct. Mater. 32 (2022) 2204137.
[4] F.Y. Chen, Z.Y. Wu, H.T. Wang, et al., Joule 5 (2021) 1704–1731.
[5] Y.Y. Li, X.C. Du, J. Xiong, et al., Small 15 (2019) 1901980.
[6] G.Q. Zhao, K. Rui, W.P. Sun, et al., Adv. Funct. Mater. 28 (2018) 1803291.
[7] Z.W. Gao, J.Y. Liu, X.W. Du, et al., Adv. Mater. 31 (2019) 1804769.
[8] H.P. Zhao, Y. Lei, Adv. Energy Mater. 10 (2020) 2001460.
[9] Z.M. Sun, L. Lin, G.B. Sun, et al., J. Am. Chem. Soc. 144 (2022) 8204–8213.
[10] M.S. You, Y. Xu, L. Zhao, et al., Appl. Catal. B: Environ. 315 (2022) 121579.
[11] Q.Z. Qian, Y.P. Li, G.Q. Zhang, et al., Adv. Mater. 31 (2019) 1901139.
[12] L. Li, X.J. Cao, G.X. Wang, et al., J. Energy Chem. 76 (2023) 195–213.
[13] X.D. Ding, W. Lin, Z.L. Xie, et al., Chem. Eng. J. 451 (2023) 138550.
[14] L. Yu, L.B. Wu, Z.F. Ren, et al., Energy Environ. Sci. 13 (2020) 3439–3446.
[15] T.F. Li, J.W. Yin, J.M. Xue, et al., Small 18 (2022) 2106592.
[16] H.W. Huang, A. Cho, J. Lee, et al., Adv. Funct. Mater. 30 (2020) 2003889.
[17] L. Yang, R.M. Liu, L.F. Jiao, Adv. Funct. Mater. 30 (2020) 1909618.
[18] Z.H. Pu, T.T. Liu, S.C. Mu, et al., Adv. Funct. Mater. 30 (2020) 2004009.
[19] Y. Jiang, Y. Li, Y. Jiang, et al., Chin. Chem. Lett. 33 (2022) 4003–4007.
[20] B. Liu, J.F. Wan, J.L. Zou, et al., Chem. Eng. J. 431 (2022) 133238.

[21] L. Yu, L.B. Wu, Z.F. Ren, et al., ACS Energy Lett. 5 (2020) 2681–2689.
[22] Y.N. Men, P. Li, W. Luo, et al., ACS Catal. 9 (2019) 3744–3752.
[23] B. Zhang, J.W. Shan, Y.Y. Li, et al., Small 18 (2022) 2106012.
[24] Y. Lin, K. Sun, C. Chen, et al., Adv. Energy Mater. 9 (2019) 1901213.
[25] L. Qi, Z.Q. Zheng, Y.L. Li, et al., Adv. Funct. Mater. 32 (2022) 2107179.
[26] Z.H. Sun, Y.K. Wang, S.J. Ding, et al., Adv. Funct. Mater. 30 (2020) 1910482.
[27] G.C. Yang, Y.Q. Jiao, H.G. Fu, et al., Adv. Mater. 32 (2020) 2000455.
[28] D. Ma, B. Hu, T.L. Liu, et al., Nat. Commun. 10 (2019) 3367.
[29] Y.J. Lin, Y. Xu, D.W. Wang, et al., J. Am. Chem. Soc. 134 (2012) 5508–5511.
[30] J. Hu, J. Wang, P. Xu, et al., Adv. Sci. 8 (2021) 2103314.
[31] D. Yan, H. Li, S. Wang, et al., Small Methods 3 (2019) 1800331.
[32] G.J. Yuan, J.L. Bai, L.L. Ren, et al., Appl. Catal. B: Environ. 284 (2021) 119693.
[33] C. Mao, J. Wang, L. Zhang, et al., Green Chem. 21 (2019) 2852–2867.
[34] L.X. Peng, L. Su, J.L. Shi, et al., Appl. Catal. B: Environ. 308 (2022) 121229.
[35] J. Sun, N.K. Guo, Q. Wang, et al., Adv. Energy Mater. 8 (2018) 1800980.
[36] N. Yao, R. Meng, W. Lou, et al., Appl. Catal. B: Environ. 277 (2020) 119282.
[37] L. Kang, C. Huang, S.C. Jun, et al., Chem. Eng. J. 390 (2020) 124643.
[38] W. Jin, J.P. Chen, G.T. Fu, et al., Small 15 (2019) 1904210.
[39] X.K. Huang, X.P. Xu, D.J. Cheng, et al., Nano Energy 68 (2020) 104332.
[40] D.J. Liu, L.T. Yang, B. Li, et al., Chem. Eng. J. 450 (2022) 137956.
[41] W.Q. Li, L. Wu, X.Z. Ren, et al., Appl. Catal. B: Environ. 303 (2022) 120849.
[42] K. He, X. Liu, X.F. Qian, et al., Angew. Chem. Int. Ed. 58 (2019) 11903–11909.
[43] X.D. Ding, Y.X. Huang, Z.L. Xie, et al., Particuology 81 (2023) 38–44.
[44] M. Wang, W.J. Zhang, X.G. Wang, et al., ACS Catal. 9 (2019) 1489–1502.
[45] J.Y. Zhang, W. Xiao, J. Ding, et al., ACS Energy Lett. 2 (2017) 1022–1028.
[46] X.F. Lu, S.L. Zhang, X.W. Lou, et al., Adv. Sci. 7 (2020) 2001178.
[47] Y. Yan, Y. Yao, Y. Liu, et al., Chin. Chem. Lett. 33 (2022) 4655–4658.
[48] S. Zhang, H. Xue, Q. Wang, et al., Small 17 (2021) 2102125.
[49] Y.R. Hao, H. Xue, Q. Wang, et al., Appl. Catal. B: Environ. 295 (2021) 120314.
[50] Z.H. Xue, H. Su, J.S. Chen, et al., Adv. Energy Mater. 7 (2017) 1602355.
[51] F.L. Yang, P.Y. Han, W. Luo, et al., Chem. Sci. 11 (2020) 12118–12123.
[52] F. Chen, Z. Zhang, W. Liang, et al., Chin. Chem. Lett. 33 (2022) 1395–1402.
[53] J. Sun, H. Xue, Q. Wang, et al., Appl. Catal. B: Environ. 313 (2022) 121429.
[54] W. Li, J. Liu, R.B. Wu, et al., Adv. Energy Mater. 11 (2021) 2102134.
[55] X.Z. Song, W.Y. Zhu, X.F. Wang, et al., ACS Appl. Mater. Interfaces 14 (2022) 33151–33160.
[56] M.Z. Gu, L. Jiang, X.J. Zhang, et al., ACS Nano 16 (2022) 15425–15439.
[57] D. Liang, C. Lian, C.Z. Li, et al., Appl. Catal. B: Environ. 268 (2020) 118417.
[58] X.N. Zheng, Y. Yao, Y. Liu, et al., Chin. Chem. Lett. 33 (2022) 1455–1458.